Water Resources Research

RESEARCH ARTICLE
10.1029/2019WR026144

Changes in Physical Properties of Everglades Peat Soils Induced by Increased Salinity at the Laboratory Scale: Implications for Changes in Biogenic Gas Dynamics

Matthew J. Sirianni[1] and **Xavier Comas**[1]

[1]Department of Geosciences, Florida Atlantic University, Boca Raton, FL, USA

Key Points:
- GPR, permeameter tests, and time-lapse photography capture the effects of salinity on peat soil biogenic gas dynamics
- Increased salinity enhances the K_H of Everglades peat soils
- Biogenic bubble production and release rates are limited by increased salinity in Everglades peat soils

Correspondence to:
M. J. Sirianni,
matt.sirianni@icloud.com

Citation:
Sirianni, M. J., & Comas, X. (2020). Changes in physical properties of Everglades peat soils induced by increased salinity at the laboratory scale: Implications for changes in biogenic gas dynamics. *Water Resources Research*, *56*, e2019WR026144. https://doi.org/10.1029/2019WR026144

Received 10 AUG 2019
Accepted 9 APR 2020
Accepted article online 28 APR 2020

Abstract Saltwater intrusion due to sea level rise is a major concern for the Florida Everglades because it may induce shifts in ecosystem productivity and physical soil properties. However, the effects of saline water intrusion into the current carbon gas dynamics of the Everglades (particularly in terms of biogenic gas production and emissions, i.e., CH_4 and CO_2) are still uncertain. In this work, we present a laboratory-based study to simulate how sea level rise may alter the physical properties (i.e., hydraulic conductivity) of peat soils from the Everglades and consequently affect the accumulation and release of biogenic gases within the peat matrix. Peat monoliths collected from the Everglades were subjected to progressive increases in salinity from a NaCl solution, and changes to the biogenic gas dynamics regime were simultaneously monitored using a combination of time-lapse ground-penetrating radar measurements, manometers, time-lapse photography, and gas traps. Physical changes to the peat matrix at each salinity interval were assessed using constant head permeameter tests. Consistent with previous research, results show that a progressive increase in salinity (from fresh to saltwater) results in (1) a progressive increase in hydraulic conductivity and (2) a progressive decrease in gas content within the peat matrix (i.e., production) and gas releases. This work has implications for better understanding the potential effects of saltwater intrusion into freshwater peatland systems in the Everglades, particularly in terms of carbon gas dynamics.

1. Introduction

Sea level rise is an increasingly important topic for many low-lying coastal areas such as South Florida. Global changes in sea level have always been a natural part of Earth's geologic history, with cycles of transgression and regression driving the geologic evolution of South Florida. Over the past 120,000 years, South Florida has experienced tremendous variations in sea level ranging from 6.6 m above (Muhs et al., 2011) to 120 m below current levels (Wanless et al., 1994). About 5,000 years ago sea level around South Florida began to stabilize, allowing the accumulation of organic material and the development of the Everglades (Gleason & Stone, 1994). Through the 20th and 21st centuries the rate of global mean sea level rise has accelerated from approximately 1.7 ± 0.3 to about 3.2 ± 0.4 mm year^{-1} (Church & White, 2006, 2011). Given its low elevation and shallow slope, the Everglades region is particularly vulnerable to changes in sea level. Regionally corrected sea level change estimates at the Virginia Key (Florida) gauge station projects that sea level could rise 0.42 m by 2050 and 1.15 m by 2100 when considering an intermediate sea level change scenario (NOAA, 2017). Given these projections, it is conceivable that previously unexposed freshwater areas of the southern Everglades will become exposed to saline water, altering hydrologic regimes, biogeochemical cycling, biological community composition, and ecosystem productivity (NOAA, 2017; Zhang et al., 2011).

The Florida Everglades is a shallow subtropical peatland located in South Florida that extends about 700,000 ha from Lake Okeechobee on the north to Florida Bay on the south and encompasses five Water Conservation Areas (WCA-1; 2A; 2B; 3A; and 3B), Everglades National Park (ENP), and the Florida Bay. The Everglades is characterized by the presence of peat (up to 4 m thick in northern portions) (Craft & Richardson, 2008), sheet flow (e.g., as connected to Lake Okeechobee and that dominated predrainage conditions), its subtropical climate, and its nutrient limitation, particularly for phosphorus. The Everglades are therefore mostly water inundated (either permanently or seasonally) over most of its entirety. Plant communities in the Everglades are dominated by dense expanses of sawgrass (*Cladium jamaicense*) sedge interspersed with water sloughs and tree islands with standing water often only a few centimeters in depth. In

the Everglades, peat soils are an amalgamation of plant biomass in various stages of decomposition (Comas, 2016), creating a complex relationship between soil structure and its physical/hydrological characteristics.

Peat soils have unique physical properties that result in distinctive hydrological conditions. For example, while total porosity ranges between 71% and 96%, effective porosity tends to be lower with values ranging from 10–40% (Comas, 2016; Rezanezhad et al., 2016). Similar to fractured geologic mediums, peat soils exhibit dual porosity (Hoag & Price, 1997), with a "mobile region" of interconnected pore spaces through which water can move relatively easily (Hayward & Clymo, 1982; Quinton et al., 2009; Rezanezhad et al., 2010), and an "immobile region" characterized by smaller open pores, and partially closed and/or dead-end pores formed by the remains of plant cells (Hayward & Clymo, 1982; Hoag & Price, 1997; Kremer et al., 2004). As peat decomposes, interparticle pore space and thus larger pores are reduced (Bragazza et al., 2008; Moore et al., 2005). Some studies of shallow peat soils show that the degree of decomposition typically increases with depth inducing a decrease in pore diameter and active porosity and thus hydraulic conductivity (K) (Rezanezhad et al., 2016). However, other studies looking at deeper peat columns (i.e., several meters) show that the change in the degree of decomposition with depth (and therefore K) is site dependent (Comas et al., 2013).

Previous studies investigating K in peat have focused on northern peatlands, leaving subtropical/tropical peatlands understudied (Baird et al., 2017; Dommain et al., 2010; Kelly et al., 2014). The disparity between geographic locations is illustrated in Table 1, which shows ranges of K values based on latitude (i.e., subtropical/tropical vs. northern/boreal), peatland type, depth of investigation, method of analysis (i.e., field methods [K_F] vs. laboratory methods [K_V; K_H]), and orientation of the laboratory measurement with regards to direction of accumulation (i.e., vertical [K_V] vs. horizontal [K_H]). Overall reported values are highly variable, ranging between 10^{-8} and 10^{-2} m s^{-1}. Northern peatland studies report field-determined K_F values ranging from 10^{-8} to 10^{-2} m s^{-1}, laboratory-determined K_H values ranging from 10^{-8} to 10^{-2} m s^{-1}, and K_V values ranging from 10^{-8} to 10^{-3} m s^{-1}. Subtropical/tropical peatland studies report the same range K_F values (i.e., 10^{-8} to 10^{-2} m s^{-1}) and lower ranges for K_H and K_V with values from ranging between 10^{-5} and 10^{-5}–10^{-4} m s^{-1} respectively. It is important to note that the ranges for K_H and K_V in subtropical/tropical peatlands are from a single study (i.e., Harrison & Weaver, 1958) and are likely not representative of the true anisotropy observed in subtropical/tropical peatlands. The wide range of reported values in Table 1 is reflective of the spatially heterogenous and anisotropic nature of peat soils. This characteristic is particularly evident, for example, in Cunliffe et al. (2013), where both K_H and K_V ranged over 6 orders of magnitude in laterally adjacent samples and up to 3 orders of magnitude in a single sample (1,000 cm^3). Additionally, determinations of K can be biased by methodologies, sample test volumes, and sampling depth and may account for some of the variability reported in Table 1.

Previous laboratory experiments (Comas & Slater, 2004; Hoag & Price, 1997; Kettridge & Binley, 2010; Ours et al., 1997) suggest that properties such as effective porosity and K of peat are sensitive to changes in fluid conductivity (e.g., NaCl solution) and thus changes in the ionic concentration of pore water located within the peat matrix, inducing the dilation of macropores and subsequent increase in effective porosity and thus hydraulic conductivity. The pore dilation process is explained by Ours et al. (1997) as interactions between a chloride solution and organic acids on the peat fiber edges that cause the organic acids to dynamically coil and compact, thus chemically dilating the macropores. The relation between K and fluid conductivity in peat soils has been observed in field-scale experiments such as van Dijk et al. (2016), showing a nearly threefold increase in K through salinization that was attributed to a combination of factors including pore dilation and decreased CH_4 production. However, the increased water salinity in some peat types may not result in changes in K (Gosch et al., 2018).

Physical properties and structure of the peat matrix are also a critical control dictating the spatial and temporal distribution of biogenic gases in peat soils (Wright et al., 2018). Biogenic gases (e.g., CH_4) generated and accumulated within the peat column can significantly decrease K (Baird & Waldron, 2003; Reynolds et al., 1992). Methanogens in the water-saturated, anaerobic zones within the peat soil column produce CH_4 (i.e., methanogenesis) as a metabolic byproduct, which accumulates within the peat matrix and is released to the atmosphere either through rapid outgassing events (ebullition), or slowly diffused upward through the matrix via pore water or vascular plants. Ebullition refers to the process by which biogenic gases are released to the atmosphere as bubbles. When the partial pressure of dissolved gases is greater than the hydrostatic

Table 1
Reported Ranges of Hydraulic Conductivity (K) Measurements of Peat Soils Across Subtropical/Tropical and Northern Systems

Nothern/boreal Peatlands							
Location	Peatland type	Depth (m)	Method of analysis	K_F (m s^{-1})	K_H (m s^{-1})	K_V (m s^{-1})	Reference
USA	Bog	0.15–0.6	Permeameter		10^{-6}–10^{-3}	10^{-7}–10^{-4}	Boelter (1965)
USA	Rasied Bog	0–3	Permeameter/Piezometer	10^{-6}–10^{-4}	10^{-7}–10^{-4}	10^{-7}–10^{-4}	Chason and Siegel (1986)
Canada	Blanket Bog	0.2–0.5	Piezometer	10^{-8}–10^{-6}			Hoag and Price (1995)
England	Fen	0–0.1	Permeameter/Infiltrometer	10^{-6}–10^{-5}		10^{-7}–10^{-5}	Baird (1997)
USA	Raised Bog	0.1–0.2	Permeameter			10^{-6}–10^{-5}	Ours et al., (1997)
Sweden	Raised Bog	0–3	Piezometer	10^{-7}–10^{-3}			Waddington and Roulet (1997)
Canada	Cut over	0–1	Permeameter/Piezometer	10^{-7}–10^{-6}	10^{-6}–10^{-5}	10^{-6}	Schlotzhauer and Price (1999)
England	Fen	0.1	Piezometer	10^{-7}–10^{-6}			Baird and Gaffney (2000)
Canada	Tundra	0–0.3	Permeameter/Tracer	10^{-5}–10^{-3}		10^{-5}–10^{-3}	Quinton et al. (2000)
Canada	Raised Bog	0–5	Piezometer		10^{-8}–10^{-3}		Fraser et al. (2001)
England	Blanket Bog	0–0.8	Piezomeer	10^{-7}–10^{-5}			Holden and Burt (2003)
England	Raised Bog	0–1.5	MCM		10^{-7}–10^{-3}	10^{-7}–10^{-3}	Beckwith et al. (2003)
USA	Raised Bog	0–11	Permeameter			10^{-6}–10^{-4}	Comas and Slater (2004)
Canada	Fen	0.5–1.5	Piezometer		10^{-8}–10^{-6}		Kennedy and Price (2005)
England	Fen	0.15–0.69	MCM/Piezometer	10^{-6}–10^{-5}	10^{-7}–10^{-5}	10^{-7}–10^{-5}	Surridge et al. (2005)
Canada	Fen	0–2	Piezometer	10^{-4}–10^{-2}		10^{-6}–10^{-5}	Hogan et al. (2006)
Germany	Fen	0.3–1.2	Permeameter		10^{-6}–10^{-5}	10^{-6}–10^{-5}	Kruse et al. (2008)
Canada	Raised Bog	0–0.05	Permeameter			10^{-4}–10^{-3}	Price et al. (2008)
Ireland	Blanket Bog	0.1–0.4	MCM		10^{-7}–10^{-4}	10^{-6}–10^{-4}	Lewis et al. (2012)
England	Blanket Bog	0–0.5	MCM		10^{-8}–10^{-2}	10^{-8}–10^{-3}	Cunliffe et al. (2013)
Sweden	Raised Bog	0–0.5	MCM		10^{-6}–10^{-2}		Morris et al. (2015)
Subtropical/tropical peatlands							
Location	Peatland type	Depth (m)	Method of analysis	K_F (m s^{-1})	K_H (m s^{-1})	K_V (m s^{-1})	Reference
USA	Everglades	0–1.2	Permeameter		10^{-5}	10^{-5}–10^{-4}	Harrison and Weaver (1958)
USA	Everglades	0.3–0.9	Piezometer	10^{-7}–10^{-5}			Harvey et al. (2000)
USA	Everglades	0.8–1.2	Piezometer	10^{-8}–10^{-4}			Harvey et al. (2004)
Malaysia	Swamp Forest	0–0.5	Piezometer	10^{-5}–10^{-3}			Sayok et al. (2007)
Peru	Forested Peatland	0–1	Piezometer	10^{-6}–10^{-3}			Kelly et al. (2014)
Panama	Swamp	0.55–0.65	Piezometer	10^{-5}–10^{-2}			Baird et al. (2017)
USA	Everglades	0–0.25	Permeameter		10^{-4}–10^{-3}		This study

pressure in the peat column, gas bubbles form (Chanton & Whiting, 1995; Lai, 2009). As other gases diffuse into the bubble the individual partial pressure of each gas in the bubble is lowered and as a result, the saturation concentration of each gas dissolved in the surrounding pore water will be lowered allowing more gas to diffuse into a growing bubble (Chanton, 2005; Glaser et al., 2016). The gas bubbles primarily consist of CH_4 and CO_2, but the exact concentrations are highly transient despite CH_4 having a lower solubility than CO_2 (Chanton, 2005; Glaser et al., 2004, 2016). The ionic strength and temperature of a solution may also affect the solubility of biogenic gases. By increasing ionic strength (e.g., NaCl concentration) or temperature, CH_4 and CO_2 become less soluble. Similarly, methanogens are limited by increasing the ionic strength of a solution (Chambers et al., 2011; Neubauer, 2013) and may reduce the clogging effects of biogenic gas bubbles on K. However, CH_4 production by methanogens may be stimulated by increased temperatures (Bachoon & Jones, 1992). While the ionic makeup of seawater is primarily composed of Na^+ and Cl^- (~86% combined), other major dissolved ions can influence soil and water biogeochemistry. For example, concentrations of SO_4^{2-} (~8% ionic makeup of seawater) are particularly important to consider under anerobic conditions because sulfate-reducing bacteria will outcompete methanogens and effectively decrease gross CH_4 production and therefore flux to the atmosphere. However, in some instances low-level saltwater additions to freshwater marsh soils may stimulate CH_4 production (Weston et al., 2011), and large CH_4 stocks have been found in saline environments (Wilson et al., 2015).

In this study, we present a laboratory-based experiment to explore how increased salinity (i.e., by adding NaCl solution) may alter the physical properties of peat soils from the Everglades and consequently affect

the accumulation and release of biogenic gases from the peat matrix. To our knowledge, this study is unique, as it combines a multidisciplinary approach that includes an array of geophysical and hydrological techniques such as ground-penetrating radar (GPR), time-lapse photography, gas chromatography, and constant head permeameter tests, which allows for inferring physical changes within the peat matrix in a minimally invasive way. Furthermore, this work also has implications for better understanding the potential impacts of sea level rise in the Florida Everglades, particularly in terms of carbon gas dynamics (i.e., bubble production, accumulation, and release of CH_4 and CO_2) and soil hydraulic properties (i.e., K).

2. Methodological Background

The GPR method is a noninvasive geophysical tool that uses electromagnetic radiation with frequencies usually between 10 MHz and 2.6 GHz to detect subsurface variations in material properties. The propagation of the radar signal through a medium is mainly dependent on the dielectric permittivity, a measure of the ability of a medium to electrically polarize that is related to the water content of a given medium. A GPR system is composed of a transmitting antenna that emits an electromagnetic wave and a receiving antenna that records the sequence of reflections from subsurface interfaces. In this study, all surveys were performed in transmission mode (as opposed to the more common reflection mode for GPR) and using the zero-offset profiling (ZOP) mode, where a transmitter and receiver antenna are placed on opposing sides of a sample at a constant separation and moved synchronously across the sample. From the known distance between the transmitter and receiver antennas and measured travel time, the velocity of the electromagnetic wave can be calculated. With this velocity (v) the bulk dielectric permittivity constant (ε_b) for the peat sample can be calculated using equation 1, where c is the speed of light in a vacuum, or 3.0×10^8 m s^{-1}.

$$v = \frac{c}{\sqrt{\varepsilon_b}} \tag{1}$$

By expressing v as ε_b, we can use it as an input into the Complex Refractive Index Model (CRIM) (equation 2), a petrophysical mixing model used here to determine the gas content of the peat.

$$\varepsilon_b^{\alpha} = \theta\varepsilon_w^{\alpha} + (1-n)\varepsilon_s^{\alpha} + (n-\theta)\varepsilon_a^{\alpha}, \tag{2}$$

where ε_w, ε_s, and ε_a are the dielectric permittivity of gas, water, and soil, respectively; n is porosity; θ is the volumetric soil water content; and α is a factor that accounts for the orientation of the electrical field and the geometrical arrangement of minerals. In this equation, gas content is expressed as ($n-\theta$) and reported as a percentage. While the GPR method is sensitive to changes in free-phase gas content within the peat matrix, it cannot determine gas composition. For that reason, the collection of gas samples and subsequent analysis via gas chromatography is needed to infer CH_4 and CO_2 concentrations and convert changes in gas content (after application of the CRIM model) into flux rates (i.e., mg CH_4 m^{-2} day^{-1}) as shown in previous studies (Wright & Comas, 2016).

The GPR method has been utilized in several studies for more than a decade to explore aspects of biogenic gas dynamics in peat soils, including field-scale studies in boreal systems to investigate both its spatial (Comas et al., 2005a, 2005b; Comas & Slater, 2013; Parsekian et al., 2011; Strack & Mierau, 2010) and temporal distribution (Comas et al., 2007; Comas et al., 2008), as well as similar studies to understand gas dynamics in subtropical systems (Comas & Wright, 2014; Wright & Comas, 2016). Laboratory-based studies have also been conducted using common offset measurements (Mustasaar & Comas, 2017) and ZOP measurements (Comas & Slater, 2007) to noninvasively monitor the internal biogenic gas dynamics of peat blocks similar to those used in this study. Compared to these studies, the uniqueness of the study presented here resides in the fact that we employ a combination of geophysical (i.e., GPR in transmission mode) and hydrological measurements on peat monoliths while inducing changes in salinity via increased concentrations of NaCl.

3. Experimental Setup

In order to evaluate the effects of increasing salinity on the carbon gas dynamics of peat soils, two peat monoliths were extracted from the surface of Water Conservation Area 3A (WCA-3A), which spans over

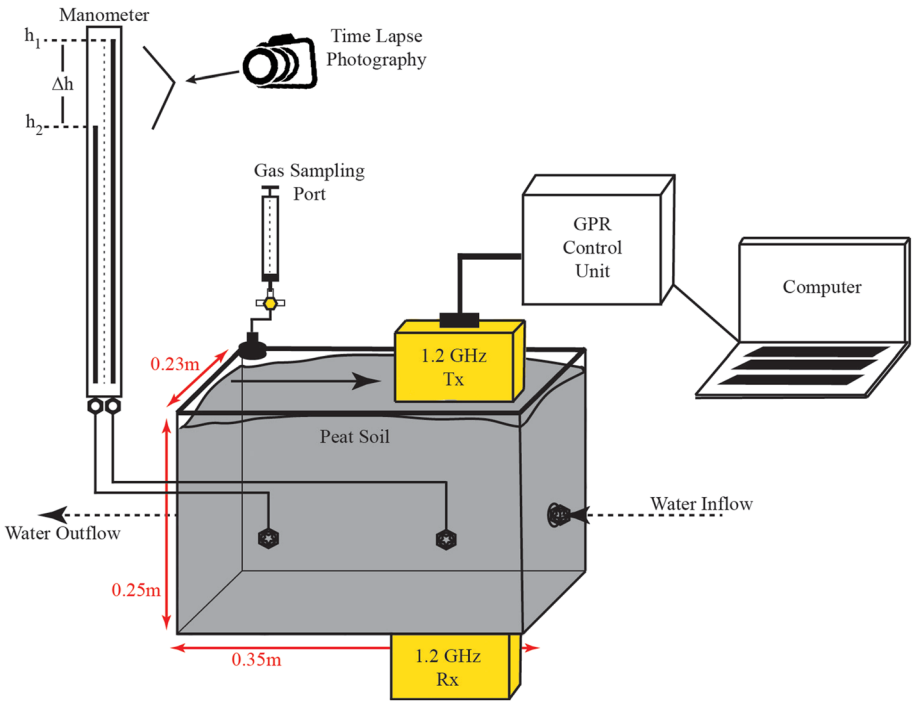

Figure 1. Schematic representation of the experimental setup. Sample vertical orientation in the lab follows that as collected in the field (i.e., top-bottom).

approximately 2,400 km^2 in the western portions of Broward and Miami-Dade Counties. Peat soils from WCA-3 are composed primarily of partially decomposed sawgrass (*Cladium jamaicense*) and water lily (*Nimphaea odorata*) and are characterized by a high organic matter ranging from 85% to ≥92% (Craft & Richardson, 2008). The monoliths were removed by first cutting and pulling back the surrounding peat and then cutting the base of the monolith with a machete. The monoliths were then placed in a plastic container and transported to the laboratory within 6 hr of extraction and stored in a light-controlled and temperature-controlled (22°C) environmental chamber. In the environmental chamber, the peat monoliths were trimmed and placed into a 0.23 × 0.35 × 0.25 m plastic sample holder creating a tight contact between the peat sample and the wall of the sample holder (Baird & Waldron, 2003), which restricted preferential flow. Clear plastic sample holders were used to visually identify preferential flow pathways (Rosa & Larocque, 2008); however, none were observed. A clear plexiglass lid was then fixed to the top of the sample holder and sealed using a silicone sealant to create an air- and water-tight environment. The sample holder was fitted with four quick disconnect valves, two of which were used for constant head permeameter tests in which K_H was measured (Figure 1). The variable K describes the ease by which a fluid can move through pore spaces of a given medium and can be calculated through Darcy's Law (equation 3).

$$Q = AK\frac{\Delta h}{L}, \tag{3}$$

where Q is the flow rate of liquid through the porous medium, A is the cross-sectional area perpendicular to flow, Δh is the change in head, and L is the length of the sample. The variable K was corrected for temperature and salinity following the approach by Gosch et al. (2018) to calculate intrinsic permeability (k) as shown in equation 4:

$$k = K\frac{\mu}{\rho g}, \tag{4}$$

where μ is the dynamic viscosity of water, ρ is the density of water, and g is the acceleration of gravity. K was then recalculated with μ and ρ for a temperature of 20°C and a fluid conductivity of 0.07 S m^{-1}, reaching differences between raw and corrected values up to 4.5%.

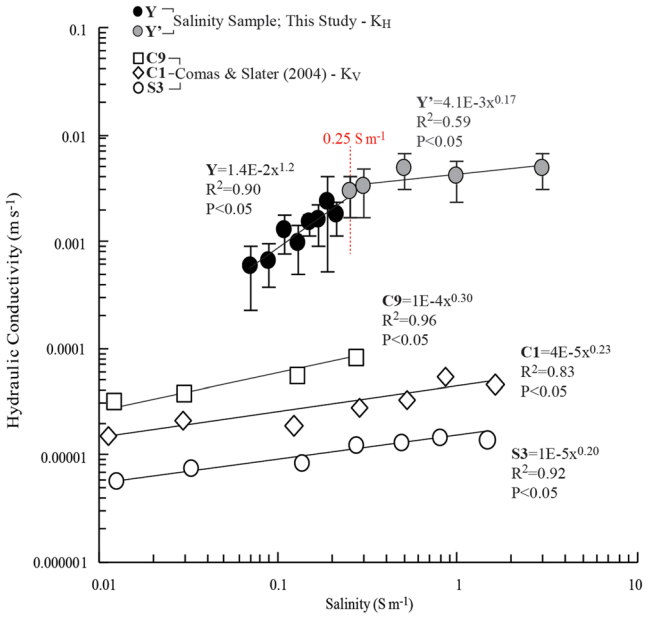

Figure 2. Dependence of horizontal hydraulic conductivity (K_H) on salinity (black and gray circles) observed in this study. K_H error bars represent ±1 standard deviation from the K_H mean calculated for each salinity interval. The red dotted line represents the salinity level (i.e., 0.25 S m^{-1}) after which the slope of K_H decreased. For comparison, the vertical hydraulic conductivity (K_V) as a function of salinity for three *Sphagnum* peat samples from Comas and Slater (2004) (open shapes) is shown.

Of the two monoliths, one was subjected to progressive increases (0.07–3 S m^{-1}) in salinity (salinity sample) by adding NaCl to deionized water, while the other was kept at a constant salinity of 0.07 S m^{-1} (control sample), mimicking conditions observed in the field. In both cases, salinity for each sample over time was confirmed using a conductivity meter. Additionally, a constant light and temperature (22°C) were maintained in both monoliths by placing samples in a controlled environmental chamber for the duration of the experiment. During each measurement period, released gas (i.e., gas accumulated at the top of the sample) was removed from the sample holder using a graduated syringe and cutoff valve sampling port and the total gas volume was recorded. Samples from the extracted gas were then processed using a Shimadzu GC-8A gas chromatographer to determine CH_4 and CO_2 concentrations. The limit of detection and limit of quantification were 0.1 and 0.3 ppm, respectively (GC-8A, Shimadzu Corporation, Kyoto, Japan). Analytical duplicates were performed for each sample achieving an average variance of 2.7% and 3.4% for CH_4 and CO_2, respectively. Ten horizontally oriented constant head permeameter tests were conducted on each sample, and an average K_H value was calculated and recorded for each measurement period. Between measurement periods, each sample holder was connected to two manometers that were photographed on a 30-min interval using time-lapse cameras.

Hydraulic head measurements have been used by others to estimate volumetric gas build up and infer gas bubble production in peat soils (Rosenberry et al., 2003). Through a known volume of gas added to the sample holder and subsequent hydraulic head response in the manometers, a calibration factor was created to infer gas volume from hydraulic head measurements. CH_4 bubble production rates (mg CH_4 m^{-2} day^{-1}) were calculated for each sampling period by considering the converted gas volume (i.e., from manometers), percentage of CH_4 (i.e., from gas chromatography), photograph time stamps, area of the sample holder, and the ideal gas law. The combination of manometers with time-lapse cameras is, to our knowledge, a unique approach to explore changes in bubble production rates over a range of salinities at high temporal resolution (i.e., minutes). Postprocessing of GPR data sets was done using ReflexW by Sandmeier Scientific. At the conclusion of the experiment, five soil specimens were taken from the salinity and control samples for porosity determination. The average porosity of both the salinity and control samples was 95% and was used to determine GPR gas content percentage through equation 2.

A linear regression was performed to determine the relation between K and salinity level in the salinity sample and to compare bubble production and release rates between the salinity and control samples. In all cases P values were calculated and reported. A Shapiro-Wilks test was also performed to assess the normality of the bubble production and release data, in order to reject the hypothesis of normality when the P value is less than or equal to 0.05. An ANOVA analysis was performed to determine if the means of the bubble production and release rates between the salinity and control samples were different at the $P < 0.05$ level.

4. Results

4.1. Hydraulic Conductivity

The observed average K_H values for the salinity sample as a function of salinity for this study are shown in Figure 2 (solid black and gray circles corresponding to K_H in the figure). Salinity was increased progressively by approximately 2 orders of magnitude from 0.07 S m^{-1} (observed field conditions) to 3 S m^{-1} (approximately seawater) during a total period of 160 days, resulting in an increase in K_H of 1 order of magnitude from 0.0006 to 0.005 m s^{-1}. To further explore the dependence of K_H on changes in salinity, we applied a least squares regression analysis and found a statistically significant linear correlation between 0.07 and 0.25 S m^{-1} (Line Y, Figure 2, black circles) ($R^2 = 0.90$; $P < 0.05$) that decreases in slope between 0.25 and

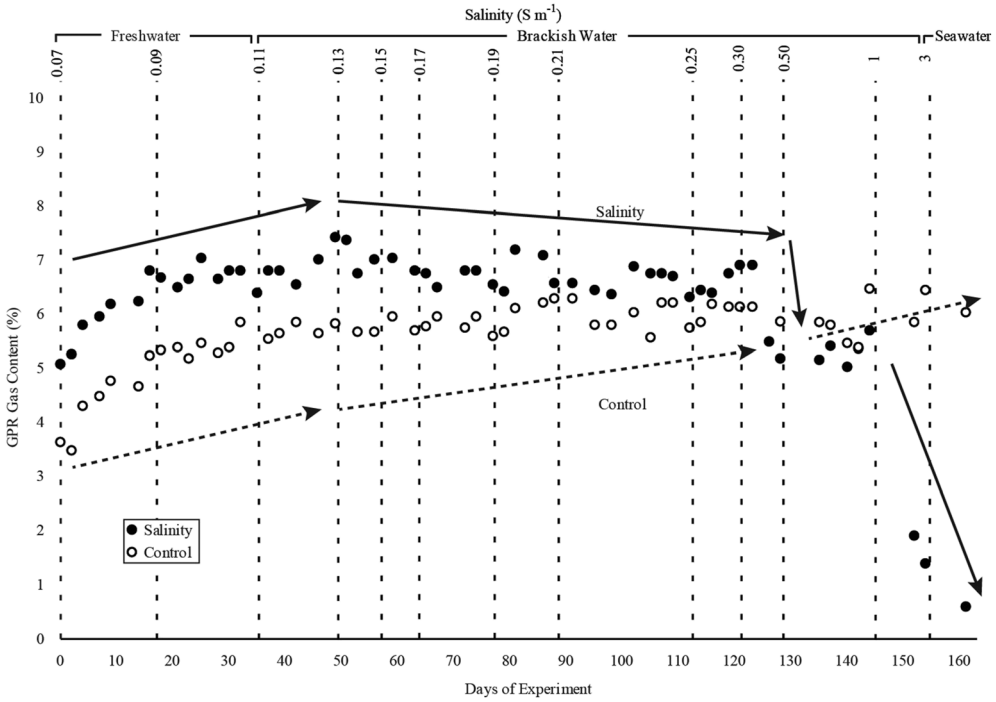

Figure 3. GPR gas contents of the salinity (black circles) and control (open circles) samples as salinity sample was exposed to progressively increasing salinity levels shown on top of graph. Arrows highlight trends observed in each sample.

3 S m^{-1} (Line Y′, Figure 2, gray circles) ($R^2 = 0.59$; $P < 0.05$). Additionally, K_H measurements on the control sample (kept at a constant salinity of 0.07 S m^{-1} for the duration of this study) resulted in an average K_H of 0.0007 ± 0.0004 m s^{-1} for the 160-day duration of the experiment. The average K_H of the control sample is consistent with the values observed in the salinity sample for the same salinity interval. In order to further compare these results with existing data sets from other peat studies, Figure 2 also shows the dependence of K_V on salinity for three *Sphagnum* peat samples from Maine as reported in Comas and Slater (2004) (open shapes) and corrected to 20°C and 0.07 S m^{-1}. In all cases, K approximates a power law dependence on fluid conductivity, showing consistency with previous studies like Comas and Slater (2004) despite the differences in depositional environment (i.e., boreal vs. subtropical peatland). As shown in Figure 2, the initial slope of K_H (slope = 1.2) is approximately four times greater than that of the K_V (slope = 0.30; 0.23; 0.20) from Comas and Slater (2004). After increasing the salinity to 0.25 S m^{-1}, the slope of K_H decreased (slope = 0.17), becoming comparable to the K_V slopes reported in Comas and Slater (2004).

4.2. Biogenic Gas Dynamics

4.2.1. Gas Chromatography

Over the course of this study, the CH_4 concentration of the released gas from the salinity sample ranged from 49% to 82%, while the control sample ranged from 54% to 78%. The CO_2 concentration of the released gas showed a decreasing trend over the study period in both the salinity and control samples. In the salinity sample CO_2 composition ranged from 1% to 17% while the control sample ranged from 6% to 14%. The variability in biogenic gas composition observed in this study is consistent with previous work by Mustasaar and Comas (2017) who found CH_4 ranged from 9% to 77% and CO_2 ranged from 2% to 18% from a peat sample collected from the Everglades. It is important to note that our gas composition analysis was limited to carbon. Additionally, this study did not quantify dissolved concentrations of CH_4 or CO_2 in the pore water of the peat monoliths.

4.2.2. GPR Gas Content

The variability in the average GPR gas content over time in the salinity and control samples was inferred through the CRIM model (equation 2) using the time-lapse set of zero-offset profile (ZOP) measurements taken over the course of the study and is shown in Figure 3. As the salinity (solid black circles) sample is

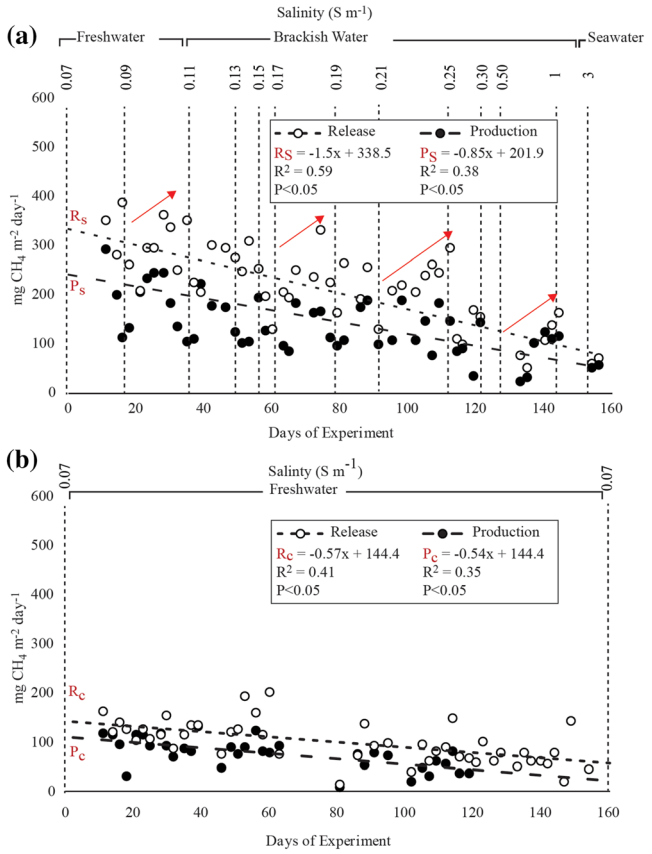

Figure 4. (a, top) Bubble production (black circles) and release (open circles) inferred from the salinity sample using manometers coupled with time-lapse photography and gas traps, respectively. Range of salinity levels is shown on top of the graph. Red arrow highlights trend observed in the data. Linear regression equation, R^2, and p value of each line are reported in the legend inlay. (b, bottom) Bubble production (black circles) and release (open circles) inferred from the control sample using monometers coupled with time-lapse photography and gas traps, respectively. Linear regression equation, R^2, and p value of each line are reported in the legend inlay.

flushed with freshwater (0.07–0.09 S m^{-1}) and slightly brackish water (i.e., between 0.11 and 0.13 S m^{-1}) gas content builds up with a consistent trend similar to the control (open circles) sample (between 5.1% and 7.4% in the salinity sample and between 3.6% and 5.8% in the control sample). This buildup is followed by a decreasing trend in the salinity sample once the water becomes more brackish (i.e., >0.13 S m^{-1}), shifting from 7.4% gas content to 6.9% when salinity reaches 0.3 S m^{-1} on Day 121. An abrupt decrease in gas content follows at this salinity during Day 126 where gas content falls from 7% to 5.5%. Between Days 130 and 145 gas content in the salinity sample shows a short increasing trend until the salinity reaches 1 S m^{-1}, when gas content suddenly drops from 6.5% to 0.6% as a salinity of 3 S m^{-1} is reached at the end of the experiment. On the other hand, the control sample (held at a constant salinity, i.e., 0.07 S m^{-1}) maintains a consistent increase in gas content reaching 6.1% gas content at the end of the study period.

4.2.3. Bubble Production and Release

Bubble production (solid black circles) and release (open circles) rates (expressed as mg CH_4 m^{-2} day $^{-1}$) in both the salinity and control samples are shown in Figures 4a and 4b, respectively. The bubble production rates for each sample were inferred by using the manometers attached to the sample holders and time-lapse photography. The release rates were inferred by evacuating all the entrapped gas beneath the sample holder lid through a cutoff valve with a graduated syringe after each sampling period. A least squares regression was used to analyze the bubble production and release rates. In the salinity sample (Figure 4a) we observed a decline in the bubble production ($P_S = -0.85$; $R^2 = 0.38$; $P < 0.05$), and a marked decline in the release ($R_S = -1.5$; $R^2 = 0.59$; $P < 0.05$) rate over time as salinity was increased from 0.07–3 S m^{-1} over the duration of the experiment. The decline in release from the salinity sample also shows a pulsating trend (illustrated by red arrows in Figure 4a) with periods of increased flux followed by sharp drops. On the other hand, the control sample (Figure 4b) shows a comparable bubble production ($P_C = -0.54$; $R^2 = 0.35$; $P < 0.05$) and release ($R_C = -0.57$; $R^2 = 0.41$; $P < 0.05$) rate decline over the duration of the study with a constant salinity of 0.07 S m^{-1} and does not show the pulsating pattern like in the salinity sample. Comparing the two samples, the slopes in the salinity sample are markedly larger than the slopes in the control sample. The overall magnitude of values for fluxes observed in the salinity sample also tends to be larger than those observed in the control sample (maximum values of 389 mg CH_4 m^{-2} day $^{-1}$ for the salinity sample vs. maximum values of 202 mg CH_4 m^{-2} day $^{-1}$ for the control sample). An ANOVA was performed and found the bubble production and release rates between the salinity and control samples to have significantly different means at the $P < 0.05$ level.

To further illustrate the differences between the salinity and control samples, Figure 5 shows the linear relationship between released gas and produced gas for each sample. The control sample shows a statistically significant positive linear relationship ($R^2 = 0.39$; $P < 0.05$) with the data tightly grouped together and centered closely around the 1:1 relationship reference line. The salinity sample also shows a statistically significant positive linear relationship ($R^2 = 0.36$; $P < 0.05$); however, the data are scattered toward higher gas releases and mainly distributed above the 1:1 relationship reference line. In both cases, however, the slope values are consistent (0.86 vs. 0.80 for the salinity and control samples, respectively) and close to 1. The graph also shows the average values for both the salinity (blue star) and the control samples (red star), which reflect the trends explained above.

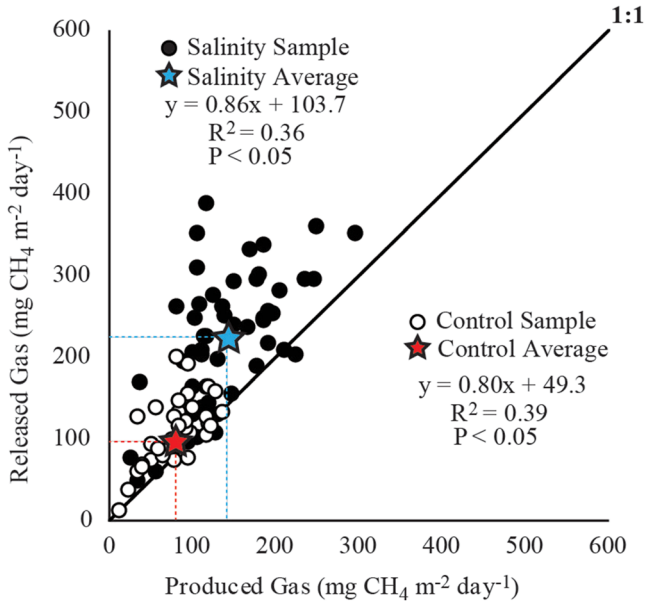

Figure 5. Produced gas versus released gas for the salinity (black circles; blue star) and control (white circles; red star) samples with average values for each sample shown as colored stars. Data are plotted against a 1:1 ratio for reference. Linear regression equation, R^2, and p value of each line are reported below the salinity and control sample legend inlay.

5. Discussion

5.1. Hydraulic Conductivity

One of the most striking results of this study relates to the progressive increase in K_H matching the increase in salinity (Figure 2). Previous work by Comas and Slater (2004) and Ours et al. (1997) showed this effect for *Sphagnum* peat soils from boreal peatlands, and our results also confirm a similar behavior for subtropical peat soils in the Everglades. The pore dilation effect is explained by the relationship between ionic strength and electrical double layer charge density in humic substances reported by others (e.g., Schmitt-Kopplin et al., 1999). As ionic strength (i.e., salinity) increases, the diffuse layer of the electrical double layer is compressed (Lesemes & Frye, 2001; Vinegar & Waxman, 1984), allowing K to increase as a result of the salinity-induced flocculation of organic acids on the peat fibers and macropore dilation (Comas & Slater, 2004; Kettridge & Binley, 2010; Ours et al., 1997). While our results compare well with previous studies that observed the effect of changes in salinity on K, other recent work has suggested that the salinity-dependent behavior of K is a function of peat chemistry and some peat may not exhibit any enhanced water flow (Gosch et al., 2018). While not considered in this study, the release and transformation of dissolved organic matter with increased salinity should be explored in future studies given the complex chemistry of humic substances and the role dissolved organic matter plays in the carbon budgets of peatlands.

While our results compare well with previous studies that observed the effect of changes in salinity on K, it is important to differentiate between K_V and K_H. For example, two of the studies (Comas & Slater, 2004; Ours et al., 1997) examined this relationship, as it pertains to K_V rather than the K_H reported in this study. As shown in Figure 2, comparing the equations for K_H (this study) and the equations for K_V (Comas & Slater, 2004), we find that the initial slope of the K_H (slope = 1.2) is approximately four to six times greater than that of the K_V (slope = 0.30; 0.23; 0.20). After increasing the salinity to 0.25 S m^{-1}, the slope of K_H decreased (slope = 0.17) and was more comparable with the slopes reported in the Comas and Slater (2004) samples. Considering that peat accretion will likely result in the peat fabric being more consistent laterally, horizontal preferential flow paths may develop as the peat decomposes (Chason & Siegel, 1986). It seems reasonable to expect this in the Everglades because the collapse of vascular plant debris, particularly from sedges (e.g., *Cladium jamaicense*), and the horizontal rhizome growth pattern of water lilies (e.g., *Nymphaea odorata*) can result in the development of a horizontal laminar structure (Boelter, 1965; Godfrey & Wooten, 1981). Additionally, sedge peat (e.g., derived from sawgrass) has a more stratified structure than *Sphagnum* peat due to the layering of dead leaves that facilitates horizontal flow of water (Dai & Sparling, 1973). Some studies in boreal systems have also found K_H several orders of magnitude greater than K_V (Beckwith et al., 2003; Chason & Siegel, 1986; Lewis et al., 2012); however, it is important to consider that K_V was not determined in this study, so this comparison is limited. Another consideration is that the samples in Comas and Slater (2004) were collected from deeper portions of the peat column (i.e., 1–10 m) than samples from our study (0.25 m) and thus may partially account for the observed difference in K magnitude between studies. The surface layer of peatlands typically has little decomposition and compaction, which results in an increased fraction of large diameter pore spaces in the surface peat matrix compared to deeper in the peat column. Moreover, *Cladium* root mats have been found to be highly permeable with $K > 10^{-3}$ m s^{-1} (Baird et al., 2004).

Another unexpected result from this study is the observed change in slope in the relation between salinity and K that occurs at around 0.25 S m^{-1} (Figure 2). We interpret this slope change to represent a threshold value where the peat matrix loses some of its ability to dilate further despite further increases in fluid conductivity. This slope change can also be interpreted as a sudden loss of the structural integrity of the peat matrix that may represent early stages of peat collapse. This is further illustrated by the releasing trend shown in Figure 4a, where the salinity sample shows a sudden increase in gas releases between 0.21 and

0.3 S m^{-1}, followed by the change in slope described above. The sudden mobilization of gas bubbles may not allow for the replacement with water and may result in the partial collapse of the peat matrix, although additional analysis is needed and warrants further investigation in future studies. We suspect that trends in the biogenic gas production and release may have also influenced our *K* results. The *K* of peat is dependent upon pore size, pore shape, and amount of gas-occupied pore space (Beckwith et al., 2003). Biogenic gases accumulation and release may affect the peat matrix, altering the movement of water and solutes in peat (Beckwith & Baird, 2001; Kellner et al., 2004) and in turn the composition and flux of biogenic gases (Rosenberry et al., 2006; Strack et al., 2005). This complex interaction is exemplified by considering that biogenic gas accumulation can produce a negative effect on water flow through the pore clogging effect (Reynolds et al., 1992). However, the combined effects of a reduction in bubble production and subsequent gas releases and pore dilation with the addition of a NaCl solution observed in this study may exert an opposing influence by increasing the total porosity and thus the proportion of active porosity available, thus enhancing *K*.

In the context of the results presented here, the slope break observed in this study occurs under (1) a slight increasing trend in GPR gas content (Figure 3), (2) an increasing trend in gas release rate followed by a sharp decline (Figure 4), and (3) an increasing trend in bubble production followed by a sharp decline (Figure 4). Given the buildup of gas in the peat matrix (shown by the GPR and bubble production data) and the increased bubble activity (shown by the gas release data), it is conceivable that pore clogging could have influenced K_H leading to the observed break in slope. After the slope change, conditions in the salinity sample are (1) decreasing GPR gas content, (2) suppressed gas release, and (3) suppressed bubble production. Following these reductions in gas content within the peat matrix and subsequent releases, *K* may have been enhanced by pore unclogging, thus accounting for the slight increase in *K* from 0.25 to 3 S m^{-1}. This explanation is consistent with other work by van Dijk et al. (2016), who concluded that a combination of factors including pore dilation and decreased CH_4 production were major controls on the observed increase in *K*. However, given the lack of replicate samples in this study, other explanations may be able to account for the observed slope break in K_H as salinity is increased and warrants future investigation.

5.2. Biogenic Gas Dynamics

This study also shows the influence of salinity on the biogenic gas dynamic of peat soils. Salinity is an important soil factor that influences a variety of soil microbial activities including methanogenesis (van Dijk et al., 2015), with previous studies demonstrating that varying concentrations of NaCl inhibit CH_4 production with reported values ranging from 0.1 S m^{-1} (Baldwin et al., 2006) to 7 S m^{-1} (Chambers et al., 2011). The large variability of this range suggests that the effects of NaCl on CH_4 production may be dependent on site-specific biogeochemical conditions, parent plant material, or soil microbial populations (e.g., Chambers et al., 2011; Neubauer et al., 2013). The influence of salinity on biogenic gas dynamics is well exemplified in Figure 3 where initially, and under freshwater conditions, the two samples behave similarly showing a progressive increase in gas content. Once brackish water is reached (around 0.13–0.15 S m^{-1}), the salinity sample almost immediately starts to show a progressive decrease in gas content, while the control sample still shows a fairly constant gas content increase. This trend culminates in the salinity sample with the sudden drop around 0.3 S m^{-1}, a plateau at 0.5 S m^{-1}, and the final drop to almost 0% gas content as the salinity sample increases to 1 S m^{-1} and beyond (demonstrated by solid black arrows in Figure 3). In contrast, the control sample maintains a consistent gas content increase for the duration of the study (demonstrated by dotted black arrows in Figure 3). The salinity sample bubble production and release rates show a fairly consistent decreasing trend as salinity is increased, even when still under freshwater conditions (Figure 4a). The gas release trend of the salinity sample (Figure 4a) shows an increase in gas release rates between 0.21 and 0.25 S m^{-1}, followed by a sudden decrease (illustrated by the red arrows in Figure 4a). A similar trend occurs again while under 0.5 S m^{-1} conditions.

The relation between produced and released gas (Figure 5) also illustrates the influence of salinity on biogenic gas dynamics. Here, the control sample data are tightly clustered around the 1:1 reference line with an average (represented by red star) production and release of 77 and 100 mg CH_4 m^{-2} day^{-1}, respectively, whereas the salinity sample deviates more from the 1:1 reference line with an average (represented by blue star) production and release of 138 and 223 mg CH_4 m^{-2} day^{-1}, respectively. One explanation for the enhanced release rate in salinity sample is that salinity-induced pore dilation may have caused the peat

matrix to release gas more readily through an increase in the connected pore spaces (i.e., effective porosity). If gas is released more readily, it would further contribute to a slowdown in gas replenishment of those pore spaces where gas has been released (when compared to the control sample), although given the lack of replication in this study other hypotheses may need to be considered and require further analysis. For instance, as salinity increases, the solubility of CH_4 decreases, and therefore, more CH_4 in the gaseous phase can be ejected from the solution in the salinity sample, which may account for the enhanced emissions observed. Conversely, decreases in temperature may increase the solubility of CH_4. The environmental chamber was kept at a constant 22°C during the entirety of the experiment, which minimized the effect of temperature dependent solubility in our study. However, in contrast to the constant chamber temperature, the average range of air temperatures in the Everglades varies seasonally with dry season (December to May) air temperatures ranging from 12°C to 25°C and wet season (May to November) air temperatures ranging from 30°C to 35°C. The higher temperatures during the wet season would generally decrease the solubility of CH_4 in solution while also promoting microbial processes like methanogenesis leading to enhanced CH_4 emissions with rising temperatures (Bachoon & Jones, 1992; Nungesser et al., 2015).

Two additional considerations may help explain the trends in gas dynamics reported above. First, the generally decreasing bubble production and release trends observed in both the salinity and control samples (Figure 4) could be due to a flushing of the labile carbon supply from the peat matrix. Groundwater flow influences gas production by regulating geochemical conditions and nutrient supply for methanogenesis (Bon et al., 2014), so it is conceivable that the constant head permeameter tests flushed some amount of labile carbon from our samples. However, without analyses of the effluent water from our samples, this is difficult to elucidate. Second, the differences between the control and salinity production and release rates on Day 0 under the same initial laboratory conditions can be explained as an effect of natural variability between the two peat samples. CH_4 gas emission from peat soils is known to vary by orders of magnitude over short distances (Lai, 2009; Sachs et al., 2010; Whalen et al., 1991). Additionally, heterogeneities in microbial activity and community composition can create hot spots for gas production and release (Mcclain et al., 2003). A recent laboratory study of an Everglades peat monolith (Mustasaar & Comas, 2017) found measured CH_4 and CO_2 flux values display a high level of spatial and temporal variability with a >1 order of magnitude range between gas flux values across the spatial extent of a small peat monolith (~0.22 m^2). Although samples from our study were collected proximal to one another, the natural variability of factors such as porosity distribution or microbial activity (among others) could account for the difference between the samples at Day 0.

Understanding the complex interactions between the physical properties and carbon dynamics of peat under increased salinity conditions is important considering current sea level rise scenarios for important ecosystems like the Everglades. While it is difficult to draw broad conclusions about the Everglades from this limited laboratory experiment, it does suggest that an increased understanding of the effect of elevated and fluctuating salinity levels on the humic chemistry of peat is needed considering that both dissolved inorganic and organic carbon are major vectors of carbon transport in the wetland carbon cycle.

6. Conclusions

In this study, we used a combination of GPR, constant head permeameter tests, time-lapse photography, and gas chromatography to investigate how increases in salinity (via NaCl solution) affects the biogenic gas dynamics of peat soils in the Everglades at the laboratory scale. Increases in salinity were found to cause an increase in K_H, a result that is consistent with other previous studies. Increases in salinity were also shown to limit biogenic gas dynamics, identifying a sharp decrease in the linear dependence of K on salinity at around 0.25 S m^{-1} that also resulted in changes to the bubble production and release rates, and suggesting a sudden change in physical properties of the peat matrix when salinity of brackish water approaches seawater. Our work therefore suggests that elevated salinity from an NaCl solution may have a persistent negative effect on matrix gas storage, bubble production, and releases. Although this laboratory study is limited through lack of replication, it suggests that as sea level rise continues to accelerate through the 21st century, it is imperative that the effects of increased salinization on the physical properties and biogenic gas dynamics regimes in freshwater peatlands are fully understood, particularly in subtropical/tropical peatlands like the Everglades.

Acknowledgments

The authors would like to thank the editor, associate editor, and four anonymous reviewers for their constructive feedback that improved the quality of this work. This work has been partially supported by ENP-NPS (AWD-001616), NOAA (GC11-337), DOE (TES 10959421), USGS (Cooperative Agreement: Carbon Dynamics of the Greater Everglades), Florida Atlantic University (FAU) Center for Environmental Studies Walter and Lalita Janke Foundation Innovations in Sustainability Science Research Fund, and the FAU Graduate Research and Inquiry Program (GRIP) Grant. We thank Dr. Matthew McClellan, Dr. William Wright, Mitchell Collins, and Mario Job for both laboratory and field support. We also thank Dr. Tara Root and the FAU Water Lab for access to various laboratory equipment. Supporting data were attached as a supplementary spreadsheet at submission and is publicly available online (at http://www.geosciences.fau.edu/geophysics-lab/data-1.php).

References

Bachoon, D., & Jones, R. D. (1992). Potential rates of methanogenesis the Everglades. *Soil Biology and Biochemistry*, *24*(1), 21–27. https://doi.org/10.1016/0038-0717(92)90237-r

Baird, A. J. (1997). Field estimation of macropore functioning and surface hydraulic conductivity in a fen peat. *Hydrological Processes*, *11*(3), 287–295. https://doi.org/10.1002/(SICI)1099-1085(19970315)11:3%3;287::AID-HYP443%3E;3.0.CO;2-L

Baird, A. J., & Gaffney, S. W. (2000). Solute movement in drained fen peat: A field tracer study in a Somerset (UK) wetland. *Hydrological Processes*, *14*(14), 2489–2503. https://doi.org/10.1002/1099-1085(20001015)14:14%3C2489::AID-HYP110%3E3.0.CO;2-Q

Baird, A. J., Low, R., Young, D., Swindles, G. T., Lopez, O. R., & Page, S. (2017). High permeability explains the vulnerability of the carbon store in drained tropical peatlands. *Geophysical Research Letters*, *44*, 1333–1339. https://doi.org/10.1002/2016GL072245

Baird, A. J., Surridge, B. W. J., & Money, R. P. (2004). An assessment of the piezometer method for measuring the hydraulic conductivity of a Cladium mariscus - Phragmites australis root mat in a Norfolk (UK) fen. *Hydrological Processes*, *18*, 275–291. https://doi.org/10.1002/hyp.1375

Baird, A. J., & Waldron, S. (2003). Shallow horizontal groundwater flow in peatlands is reduced by bacteriogenic gas production. *Geophysical Research Letters*, *30*(20), 2043. https://doi.org/10.1029/2003GL018233

Baldwin, D. S., Rees, G. N., Mitchell, A. M., Watson, G., & Williams, J. (2006). The short-term effects of salinization on anaerobic nutrient cycling and microbial community structure in sediment from a freshwater wetland. *Wetlands*, *26*(2), 455–464. https://doi.org/10.1672/0277-5212(2006)26[455:TSEOSO]2.0.CO;2

Beckwith, C. W., & Baird, A. J. (2001). Effect of biogenic gas bubbles on water flow through poorly decomposed blanket peat. *Water Resources Research*, *37*(3), 551–558. https://doi.org/10.1029/2000WR900303

Beckwith, C. W., Baird, A. J., & Heathwaite, A. L. (2003). Anisotropy and depth-related heterogeneity of hydraulic conductivity in a bog peat. I: Laboratory measurements. *Hydrological Processes*, *17*(1), 89–101. https://doi.org/10.1002/hyp.1116

Boelter, D. H. (1965). Hydraulic conductivity of peats. *Soil Science*, *100*(4), 227–231. https://doi.org/10.1097/00010694-196510000-00001

Bon, C. E., Reeve, A. S., Slater, L., & Comas, X. (2014). Using hydrologic measurements to investigate free-phase gas ebullition in a Maine peatland, USA. *Hydrology and Earth System Sciences*, *18*(3), 953–965. https://doi.org/10.5194/hess-18-953-2014

Bragazza, L., Buttler, A., Siegenthaler, A., & Mitchell, E. A. D. (2008). Plant litter decomposition and nutrient release in peatlands. In A. J. Baird, L. R. Belyea, X. Comas, A. S. Reeve, & L. D. Slater (Eds.), *Carbon cycling in northern peatlands, geophysical monograph series* (Vol. 184, pp. 99–110). Washington, DC: American Geophysical Union.

Chambers, L. G., Reddy, K. R., & Osborne, T. Z. (2011). Short-term response of carbon cycling to salinity pulses in a freshwater wetland. *Soil Science Society of America Journal*, *75*(5), 2000–2007. https://doi.org/10.2136/sssaj2011.0026

Chanton, J. P. (2005). The effect of gas transport on the isotope signature of methane in wetlands. *Organic Geochemistry*, *36*(5), 753–768. https://doi.org/10.1016/j.orggeochem.2004.10.007

Chanton, J. P., & Whiting, G. J. (1995). Trace gas exchange in freshwater and coastal marine environments: Ebullition and transport by plants. In *Biogenic Trace Gases: Measuring Emissions from Soil and Water*, (pp. 98–125). John Wiley & Sons.

Chason, D. B., & Siegel, D. I. (1986). Hydraulic conductivity and related physical properties of peat, Lost River Peatland, northern Minnesota. *Soil Science*, *142*(2), 91–99. https://doi.org/10.1097/00010694-198608000-00005

Church, J. A., & White, N. J. (2006). A 20th century acceleration in global sea-level rise. *Geophysical Research Letters*, *33*, L01602. https://doi.org/10.1029/2005GL024826

Church, J. A., & White, N. J. (2011). Sea-level rise from the late 19th to the early 21st century. *Surveys in Geophysics*, *32*(4–5), 585–602. https://doi.org/10.1007/s10712-011-9119-1

Comas, X. (2016). Peat. In M. J. Kennish (Ed.), *Encyclopedia of estuaries, encyclopeida of earth sciences series*, (pp. 476–480). Netherlands: Springer.

Comas, X., Kettridge, N., Binley, A., Slater, L., Parsekian, A., Baird, A. J., et al. (2013). The effect of peat structure on the spatial distribution of biogenic gases within bogs. *Hydrological Processes*, *28*(22), 5483–5494. https://doi.org/10.1002/hyp.10056

Comas, X., & Slater, L. (2004). Low-frequency electrical properties of peat. *Water Resources Research*, *40*, W12414. https://doi.org/10.1029/2004WR003534

Comas, X., & Slater, L. (2007). Evolution of biogenic gasses in peat blocks inferred from non-invasive dielectric permittivity measurements. *Water Resources Research*, *43*, W05424. https://doi.org/10.1029/2006WR005562

Comas, X., & Slater, L. (2013). Noninvasive field-scale characterization of gaseous-phase methane dynamics in peatlands using the ground-penetrating radar method. In A. J. Baird, L. R. Belyea, X. Comas, A. S. Reeve, & L. D. Slater (Eds.), *Carbon Cycling in Northern Peatlands, Geophysical Monograph Series*, (Vol. 184, pp. 159–171). Washington, DC: American Geophysical Union.

Comas, X., Slater, L., & Reeve, A. (2005a). Spatial variability in biogenic gas accumulations in peat soils is revealed by ground penetrating radar (GPR). *Geophysical Research Letters*, *32*, L08401. https://doi.org/10.1029/2004GL022297

Comas, X., Slater, L., & Reeve, A. (2005b). Stratigraphic controls on pool formation in a domed bog inferred from ground penetrating radar (GPR). *Journal of Hydrology*, *315*(1–4), 40–51. https://doi.org/10.1016/j.jhydrol.2005.04.020

Comas, X., Slater, L., & Reeve, A. (2007). In situ monitoring of free-phase gas accumulation and release in peatlands using ground penetrating radar (GPR). *Geophysical Research Letters*, *34*, L06402. https://doi.org/10.1029/2006GL029014

Comas, X., Slater, L., & Reeve, A. (2008). Seasonal geophysical monitoring of biogenic gases in a northern peatland: Implications for temporal and spatial variability in free phase gas production rates. *Journal of Geophysical Research.*, *113*, G01012. https://doi.org/10.1029/2007JG000575

Comas, X., & Wright, W. (2014). Investigating carbon flux variability in subtropical peat soils of the Everglades using hydrogeophysical methods. *Journal of Geophysical Research: Biogeosciences*, *119*, 1506–1519. https://doi.org/10.1002/2013JG002601

Craft, C. B., & Richardson, C. J. (2008). Soil characteristics of the everglades peatland. In C. J. Richardson (Ed.), *The everglades experiments: Lessons for ecosystem restoration, ecological book series*, (Vol. 201, pp. 59–73). New York: Springer-Verlag.

Cunliffe, A. M., Baird, A. J., & Holden, J. (2013). Hydrological hotspots in blanket peatlands: Spatial variation in peat permeability around a natural soil pipe. *Water Resources Research*, *49*, 5342–5354. https://doi.org/10.1002/wrcr.20435

Dai, T. S., & Sparling, J. H. (1973). Measurement of hydraulic conductivity of peats. *Canadian Journal of Soil Science*, *53*, 21–26. https://doi.org/10.4141/cjss73-003

Dommain, R., Couwenberg, J., & Joosten, H. (2010). Hydrological self-regulation of domed peatlands in south-east Asia and consequences for conservation and restoration. *Mires and Peat*, *6*(5), 1–17.

Fraser, C. J. D., Roulet, N. T., & Moore, T. R. (2001). Hydrology and dissolved organic carbon biogeochemistry in an ombrotrophic bog. *Hydrological Processes*, *15*(16), 3151–3166. https://doi.org/10.1002/hyp.322

Glaser, P. H., Chanton, J. P., Morin, P., Rosenberry, D. O., Siegel, D. I., Ruud, O., et al. (2004). Surface deformations as indicators of deep ebullition fluxes in a large northern peatland. *Global Biogeochemical Cycles*, *18*(1), GB1003. https://doi.org/10.1029/2003GB002069

Glaser, P. H., Siegel, D. I., Chanton, J. P., Reeve, A. S., Rosenberry, D. O., Corbett, J. E., et al. (2016). Climatic drivers for multi-decadal shifts in solute transport and methane production zones within a large peat basin. *Global Biogeochemical Cycles*, *30*(11), 1578–1598. https://doi.org/10.1002/2016GB005397

Gleason, P. J., & Stone, P. (1994). Age, origin, and landscape evolution of the Everglades peatland. In S. M. Davis & J. C. Ogden (Eds.), *Everglades: The ecosystem and its restoration* (pp. 149–199). Delray Beach: St. Lucie Press.

Godfrey, R. K., & Wooten, J. W. (1981). *Aquatic and wetland plants of the southeastern United States*. Athens, Georgia, USA: University of Georgia Press.

Gosch, L., Janssen, M., & Lennartz, B. (2018). Impact of the water salinity on the hydraulic conductivity of fen peat. *Hydrological Processes*, *32*(9), 1214–1222. https://doi.org/10.1002/hyp.11478

Harrison, H. A., & Weaver, D. S. (1958). Some drainage characteristics of a cultivated organic soil in the Everglades. *Proceedings-Soil and Crop Science Society of Florida*, 184–192.

Harvey, J. W., Jonah, M., Mooney, R. H., & Choi, J. (2000). Interaction between ground water and surface water in Taylor slough and vicinity, Everglades National Park, South Florida: Study Methods and Appendixes. *U.S. Geological Survey Open-File Report 00–483*. Retrieved from https://pubs.er.usgs.gov/publication/ofr00483

Harvey, J. W., Krupa, S. L., & Krest, J. M. (2004). Ground water recharge and discharge in the central everglades. *Ground Water*, *42*(7), 1090–1102. https://doi.org/10.1111/j.1745-6584.2004.tb02646.x

Hayward, P. M., & Clymo, R. S. (1982). Profiles of water content and pore size in Sphagnum peat, and their relation to peat bog ecology. *Proceedings of the Royal Society London B*, *215*(1200). https://doi.org/10.1098/rspb.1982.0044

Hoag, R. S., & Price, J. S. (1995). A field-scale, natural gradient solute transport experiment in peat at a Newfoundland blanket bog. *Journal of Hydrology*, *172*(1–4), 171–184. https://doi.org/10.1016/0022-1694(95)02696-M

Hoag, R. S., & Price, J. S. (1997). The effects of matrix diffusions on solute transport and retardation in undisturbed peat in laboratory columns. *Journal of Contaminant Hydrology*, *28*(3), 193–205. https://doi.org/10.1016/S0169-7722(96)00085-X

Hogan, J. M., van der Kamp, G., Barbour, S. L., & Schmidt, R. (2006). Field methods for measuring hydraulic properties of peat deposits. *Hydrological Processes*, *20*(17), 3635–3649. https://doi.org/10.1002/hyp.6379

Holden, J., & Burt, T. P. (2003). Hydraulic conductivity in upland blanket peat: Measurement and variability. *Hydrological Processes*, *17*(6), 1227–1237. https://doi.org/10.1002/hyp.1182

Kellner, E., Price, J. S., & Waddington, J. M. (2004). Pressure variations in peat as a result of gas bubble dynamics. *Hydrological Processes*, *18*(13), 2599–2605. https://doi.org/10.1002/hyp.5650

Kelly, T. J., Baird, A. J., Roucoux, K. H., Baker, T. R., Honorio Coronado, E. N., Ríos, M., & Lawson, I. T. (2014). The high hydraulic conductivity of three wooded tropical peat swamps in northeast Peru: Measurements and implications for hydrological function. *Hydrological Processes*, *28*(9), 3373–3387. https://doi.org/10.1002/hyp.9884

Kennedy, G. W., & Price, J. S. (2005). A conceptual model of volume-change controls on the hydrology of cutover peats. *Journal of Hydrology*, *302*(1–4), 13–27. https://doi.org/10.1016/j.jhydrol.2004.06.024

Kettridge, N., & Binley, A. (2010). Evaluating the effect of using artificial pore water on the quality of laboratory hydraulic conductivity measurements of peat. *Hydrological Processes*, *24*(18), 2629–2640. https://doi.org/10.1002/hyp.7693

Kremer, C., Pettolino, F., Bacic, A., & Drinnan, A. (2004). Distribution of cell wall components in Sphagnum hyaline cells and in liverwort and hornwort elaters. *Planta*, *219*(6), 1023–1035. https://doi.org/10.1007/s00425-004-1308-4

Kruse, J., Lennartz, B., & Leinweber, P. (2008). A modified method for measuring saturated hydraulic conductivity and anisotropy of peat samples. *Wetlands*, *28*(2), 527–531. https://doi.org/10.1672/07-153.1

Lai, D. Y. F. (2009). Methane dynamics in northern peatlands: A review. *Pedosphere*, *19*(4), 409–421. https://doi.org/10.1016/S1002-0160(09)00003-4

Lesemes, D. P., & Frye, K. M. (2001). Influence of pore fluid chemistry on the complex conductivity and induced-polarization responses of Berea sandstone. *Journal of Geophysical Research*, *106*(B3), 4079–4090. https://doi.org/10.1029/2000JB900392

Lewis, C., Albertson, J. D., Xu, X., & Kiely, G. (2012). Spatial variability of hydraulic conductivity and bulk density along a blanket peatland hillslope. *Hydrological Processes*, *26*(10), 1527–1537. https://doi.org/10.1002/hyp.8252

Mcclain, M. E., Boyer, E. W., Dent, C. L., Gergel, S. E., Grimm, N. B., Groffman, P. M., et al. (2003). Biogeochemical hot spots and hot moments at the interface of terrestrial and aquatic ecosystems. *Ecosystems*, *6*, 301–312. https://doi.org/10.1007/s10021-003-0161-9

Moore, T. R., Trofymow, J. A., Siltanen, M., Prescott, C., & CIDET Working Group (2005). Patterns of decomposition and carbon, nitrogen, and phosphorus dynamics of litter in upland forest and peatland sites in central Canada. *Canadian Journal of Forest Research*, *35*(1), 133–142. https://doi.org/10.1139/x04-149

Morris, P. J., Baird, A. J., & Belyea, L. R. (2015). Bridging the gap between models and measurements of peat hydraulic conductivity. *Water Resources Research*, *51*, 5353–5364. https://doi.org/10.1002/2015WR017264

Muhs, D. R., Simmons, K. R., Schumann, R. R., & Halley, R. B. (2011). Sea-level history of the past two interglacial periods: New evidence from U-series dating of reef corals from south Florida. *Quaternary Science Reviews*, *30*(5–6), 570–590. https://doi.org/10.1016/j.quascirev.2010.12.019

Mustasaar, M., & Comas, X. (2017). Spatiotemporal variability in biogenic gas dynamics in a subtropical peat soil at the laboratory scale is revealed using high-resolution ground-penetrating radar. *Journal of Geophysical Research: Biogeosciences*, *122*, 2219–2232. https://doi.org/10.1002/2016JG003714

Neubauer, S. C. (2013). Ecosystem responses of a tidal freshwater marsh experiencing saltwater intrusion and altered hydrology. *Estuaries and Coasts*, *36*(3), 491–507. https://doi.org/10.1007/s12237-011-9455-x

NOAA (2017). Global and regional sea level rise scenarios for the United States. *Technical Report NOS CO-OPS 083*. Retrieved from https://tidesandcurrents.noaa.gov/publications/techrpt83_Global_and_Regional_SLR_Scenarios_for_the_US_final.pdf

Nungesser, M., Saunders, C., Coronado-Molina, C., Obeysekera, J., Johnson, J., McVoy, C., & Benscoter, B. (2015). Potential effects of climate change on Florida's Everglades. *Environmental Management*, *55*(4), 824–835. https://doi.org/10.1007/s00267-014-0417-5

Ours, D. P., Siegel, D. I., & Glaser, P. H. (1997). Chemical dilation and the dual porosity of humified bog peat. *Journal of Hydrology*, *197*(1–4), 348–360. https://doi.org/10.1016/S0022-1694(96)03247-7

Parsekian, A. D., Comas, X., Slater, L., & Glaser, P. H. (2011). Geophysical evidence for the lateral distribution of free phase gas at the peat basin scale in a large northern peatland. *Journal of Geophysical Research*, *116*, G03008. https://doi.org/10.1029/2010JG001543

Price, J. S., Whittington, P. N., Elrick, D. E., Strack, M., Brunet, N., & Faux, E. (2008). A method to determine unsaturated hydraulic conductivity in living and undecomposed moss. *Soil Science Society of America Journal*, *72*(2), 487–491. https://doi.org/10.2136/sssaj2007.0111N

Quinton, W. L., Elliot, T., Price, J. S., Rezanezhad, F., & Heck, R. (2009). Measuring physical and hydraulic properties of peat from X-ray tomography. *Geoderma*, *153*(1–2), 269–277. https://doi.org/10.1016/j.geoderma.2009.08.010

Quinton, W. L., Gray, D. M., & Marsh, P. (2000). Subsurface drainage from hummock-covered hillslopes in the arctic tundra. *Journal of Hydrology*, *237*(1–2), 113–125. https://doi.org/10.1016/S0022-1694(00)00304-8

Reynolds, W. D., Brown, D. A., Mathur, S. P., & Overend, R. P. (1992). Effect of in-situ gas accumulation on the hydraulic conductivity of peat. *Soil Science*, *153*(5), 397–408. https://doi.org/10.1097/00010694-199205000-00007

Rezanezhad, F., Price, J. S., Quinton, W. L., Lennartz, B., Milojevic, T., & Van Cappellen, P. (2016). Structure of peat soils and implications for water storage, flow and solute transport: A review update for geochemists. *Chemical Geology*, *429*, 75–84. https://doi.org/10.1016/j.chemgeo.2016.03.010

Rezanezhad, F., Quinton, W. L., Price, J. S., Elrick, D., Elliot, T., & Shook, K. R. (2010). Influence of pore size and geometry on peat unsaturated hydraulic conductivity computed from 3D computed tomography image analysis. *Hydrological Processes*, *24*(21), 2983–2994. https://doi.org/10.1002/hyp.7709

Rosa, R., & Larocque, M. (2008). Investigating peat hydrological properties using field and laboratory methods: Application to the Lanoraie peatland complex (southern Quebec, Canada). *Hydrological Processes*, *22*(12), 1866–1875. https://doi.org/10.1002/hyp.6771

Rosenberry, D. O., Glaser, P. H., & Siegel, D. I. (2006). The hydrology of northern peatlands as affected by biogenic gas: Current developments and research needs. *Hydrological Processes*, *20*(17), 3601–3610. https://doi.org/10.1002/hyp.6377

Rosenberry, D. O., Glaser, P. H., Siegel, D. I., & Weeks, E. P. (2003). Use of hydraulic head to estimate volumetric gas content and ebullition flux in northern peatlands. *Water Resources Research*, *39*(3), 1066. https://doi.org/10.1029/2002WR001377

Sachs, T., Giebels, M., Boike, J., & Kutzbach, L. (2010). Environmental controls on CH_4 emissions from polygonal tundra on the microsite scale in the Lena river delta, Siberia. *Global Change Biology*, *14*(6), 1395–1408. https://doi.org/10.1111/j.1365-2486.2010.02232x

Sayok, A. K., Nik, A. R., Melling, L., Samad, R. A., & Efransjah, E. (2007). Some characteristics of peat in Loagan Bunut National Park, Sarawak, Malaysia. *Carbon-Climate-Human Interactions on Tropical Peatland: Carbon Pools, Fire, Mitigation, Restoration and Wise Use, Edited by: Rieley, JO, Banks, CJ, and Ragjagukguk, B., Proceedings of the International Symposium and Workshop on Tropical Peatland, Yogyakar*, (October), 95–100.

Schlotzhauer, S. M., & Price, J. S. (1999). Soil water flow dynamics in a managed cutover peat field, Quebec: Field and laboratory investigations. *Water Resources Research*, *35*(12), 3675–3683. https://doi.org/10.1029/1999WR900126

Schmitt-Kopplin, P., Freitag, D., Kettrup, A., Hertkorn, N., Schoen, U., Klocking, R., et al. (1999). Analysis of synthetic humic substances for medical and environmental application s by capillary zone electrophoresis. *Analusis*, *27*(5), 390–395. https://doi.org/10.1051/analusis:1999270390

Strack, M., Kellner, E., & Waddington, J. M. (2005). Dynamics of biogenic as bubbles in peat and their effects on peatland biogeochemistry. *Global Biogeochemical Cycles.*, *19*(1), GB1003. https://doi.org/10.1029/2004GB002330

Strack, M., & Mierau, T. (2010). Evaluating spatial variability of free-phase gas in peat using ground-penetrating radar and direct measurement. *Journal of Geophysical Research*, *115*, G02010. https://doi.org/10.1029/2009JG001045

Surridge, B. W. J., Baird, A. J., & Heathwaite, A. L. (2005). Evaluating the quality of hydraulic conductivity estimates from piezometer slug tests in peat. *Hydrological Processes*, *19*(6), 1227–1244. https://doi.org/10.1002/hyp.5653

van Dijk, G., Nijp, J. J., Metselaar, K., Lamers, L. P. M., & Smolders, A. J. P. (2016). Salinty-induced increase of the hydraulic conductivity in the hyporheic zone of coastal wetlands. *Hydrological Processes*, *31*(4), 880–890. https://doi.org/10.1002/hyp.11068

van Dijk, G., Smolders, A. J. P., Loeb, R., Bout, A., Roelofs, J. G. M., & Lamers, L. P. M. (2015). Salinization of coastal freshwater wetlands; effects of constant versus fluctuating salinity on sediment biogeochemistry. *Biogeochemistry*, *126*(1–2), 71–84. https://doi.org/10.1007/s10533-015-0140-1

Vinegar, H. J., & Waxman, M. H. (1984). Induced polarization of shaly sands. *Geophysics*, *49*(8), 1267–1287. https://doi.org/10.1190/1.1441755

Waddington, J. M., & Roulet, N. T. (1997). Groundwater flow and dissolved carbon movement in a boreal peatland. *Journal of Hydrology*, *191*(1–4), 122–138.

Wanless, H. R., Parkinson, R. W., & Tedesco, L. P. (1994). Sea level control on stability of Everglades wetlands. In S. M. Davis, & J. C. Ogden (Eds.), *Everglades: The ecosystem and its restoration* (pp. 199–225). Delray Beach: St. Lucie Press.

Weston, N. B., Vile, M. A., Neubauer, S. C., & Velinsky, D. J. (2011). Accelerated microbial organic matter mineralization following salt-water intrusion into tidal freshwater marsh soils. *Biogeochemistry*, *102*, 135–151. https://doi.org/10.1007/s10533-010-9427-4

Whalen, S. C., Reeburgh, W. S., & Kizer, K. S. (1991). Methane consumption and emission by taiga. *Biogeochemical Cycles.*, *5*(3), 261–273. https://doi.org/10.1029/91GB01303

Wilson, B. J., Mortazavi, B., & Kiene, R. P. (2015). Spatial and temporal variability in carbon dioxide and methane exchange at three coastal marshes along a salinity gradient in a northern Gulf of Mexico estuary. *Biogeochemistry*, *123*(3), 329–347. https://doi.org/10.1007/s10533-015-0085-4

Wright, W., & Comas, X. (2016). Estimating methane gas production in peat soils of the Florida Everglades using hydrogeophysical methods. *Journal of Geophysical Research: Biogeosciences*, *121*, 1190–1202. https://doi.org/10.1002/2015JG003246

Wright, W., Ramirez, J. A., & Comas, X. (2018). Methane ebullition from subtropical peat: Testing an ebullition model reveals the importance of pore structure. *Geophysical Research Letters.*, *45*, 6992–6999. https://doi.org/10.1029/2018GL077352

Zhang, K., Dittmar, J., Ross, M., & Bergh, C. (2011). Assessment of sea level rise impacts on human population and real property in the Florida Keys. *Climatic Change*, *107*(1–2), 129–146. https://doi.org/10.1007/s10584-011-0080-2